

Electrical characterization of low defect density nonpolar (11 $\bar{2}$ 0) *a*-plane GaN grown with sidewall lateral epitaxial overgrowth (SLEO)

Bilge Imer^{a)} and Benjamin Haskell

University of California–Santa Barbara, Materials Department, Santa Barbara, California 93106; and Exploratory Research for Advanced Technology, Japan Science and Technology Corporation (NICP/ERATO JST) Group, University of California–Santa Barbara, Santa Barbara, California 93106

Siddharth Rajan, Stacia Keller, and Umesh K. Mishra

University of California–Santa Barbara, Electrical and Computer Engineering Department, Santa Barbara, California 93106

Shuji Nakamura

University of California–Santa Barbara, Materials Department, Santa Barbara, California 93106; Exploratory Research for Advanced Technology, Japan Science and Technology Corporation (NICP/ERATO JST) Group, University of California–Santa Barbara, Santa Barbara, California 93106; and University of California–Santa Barbara, Electrical and Computer Engineering Department, Santa Barbara, California 93106

James S. Speck

University of California–Santa Barbara, Materials Department, Santa Barbara, California 93106; and Exploratory Research for Advanced Technology, Japan Science and Technology Corporation (NICP/ERATO JST) Group, University of California–Santa Barbara, Santa Barbara, California 93106

Steven P. DenBaars

University of California–Santa Barbara, Materials Department, Santa Barbara, California 93106; Exploratory Research for Advanced Technology, Japan Science and Technology Corporation (NICP/ERATO JST) Group, University of California–Santa Barbara, Santa Barbara, California 93106; and University of California–Santa Barbara, Electrical and Computer Engineering Department, Santa Barbara, California 93106

(Received 4 October 2007; accepted 15 November 2007)

We studied the effect of extended defects on electrical characteristics of Si doped *n*-type nonpolar *a*-plane GaN films. The *n*-type GaN layers were grown on co-loaded reduced defect density sidewall lateral epitaxial overgrowth (SLEO) *a*-plane GaN templates and high defect density planar *a*-plane GaN templates by metalorganic chemical vapor deposition (MOCVD). The highest conductivity value was observed at the carrier concentration of $1.05 \times 10^{19} \text{ cm}^{-3}$ as $261.12 \text{ cm}^2/\text{Vs}$ for SLEO *a*-GaN and $106.77 \text{ cm}^2/\text{Vs}$ for the planar *a*-plane GaN samples. At the same doping level, the carrier compensation for SLEO samples was $\sim 12\%$ less than planar samples.

I. INTRODUCTION

When nitrides grown along nonpolar directions, such as *a*-(11 $\bar{2}$ 0) and *m*-(1 $\bar{1}$ 00) planes, it is possible to eliminate polarization fields and polarization related detrimental effects and establish the transitions between conduction and valence bands with flat-band conduction in nonpolar quantum wells.^{1–3} However, in nonpolar III–nitride epitaxial films, the extended defect densities are fairly high. The main extended defects are threading dislocations (TD) and stacking faults (SF) in current state-of-the-art nonpolar GaN films. Planar *a*-(11 $\bar{2}$ 0) plane GaN films have at least 1–2 orders of magnitude higher TD

densities compared with planar *c*-(0001)-plane GaN films. Planar *c*-plane GaN films can be grown at atmospheric pressures, while planar *a*-GaN films have to be grown at low pressures (<76 Torr). Over 76 Torr, surface faceting and degradation in crystal quality was unavoidable, and over 300 Torr, there was no dominant *a*-plane GaN surface present.⁴ The range of metalorganic chemical vapor deposition (MOCVD) growth parameters to sustain planar *a*-plane films (growth “window”) is narrow and highly sensitive to changes in growth variables, such as reactor pressure and precursor flow rates. The limited growth window of *a*-plane films was associated with presence of high defect densities. Being restricted in the low-pressure regime for *a*-plane GaN creates the risk of incorporating unintentional carbon impurities. Unintentional incorporation of such an impurity in GaN can cause carrier compensation when it is a shallow acceptor,

^{a)}Address all correspondence to this author.

e-mail: bilge@engineering.ucsb.edu

DOI: 10.1557/JMR.2008.0069

degrading electrical and optical characteristics of the devices. It was proved that carbon is the main reason for carrier compensation because it acts as acceptor in nitrogen vacancy sites, C_N .⁵ Normally as the carrier concentration decreases, mobilities should increase. However, under a certain level of carrier concentration ($2 \times 10^{17} \text{ cm}^{-3}$ for *c*-plane GaN and $2 \times 10^{18} \text{ cm}^{-3}$ for *a*-plane GaN because of higher carbon incorporation at lower pressures), the mobility values drop due to carrier compensation.

The first mobility values for MOCVD grown *n*-type nonpolar *a*-plane GaN was reported by Craven et al.⁶ as $109 \text{ cm}^2/\text{Vs}$ at a carrier concentration of $1.8 \times 10^{19} \text{ cm}^{-3}$ with a residual acceptor concentration of $\sim(1-2) \times 10^{18} \text{ cm}^{-3}$. The low-pressure growth conditions required to obtain coalesced *a*-plane GaN promoted carbon incorporation into the films at $\sim(8-9) \times 10^{17} \text{ cm}^{-3}$. Therefore at doping levels below $\sim(1-2) \times 10^{18} \text{ cm}^{-3}$, the films were highly resistive. In 2005, Kusakabe et al.⁷ reported mobility values of $220 \text{ cm}^2/\text{Vs}$ for an electron concentration of $1.1 \times 10^{18} \text{ cm}^{-3}$.

In addition to carbon, defects, such as dislocation related states and Ga vacancies, in the material can be held accountable for compensation. Also, at higher carrier concentrations these impurities and defects act as scattering centers, further degrading the Hall mobilities.^{8,9} TDs act as nonradiative recombination centers, i.e., they behave as acceptors in *n*-type material and as donors in *p*-type material with acceptor- and donor-like localized traps.¹⁰ They also act as carrier charge sinks, causing ineffective doping.¹¹ Therefore, it is essential to reduce these defect densities and electrically characterize them to improve on device performance.

In this article, we aim to demonstrate the effect of extended defect densities on electrical performance of nonpolar *a*-plane GaN. We used the sidewall lateral epitaxial overgrowth (SLEO) method to reduce TD and SF densities.¹² Essentially, SLEO is a technique to reduce the extended defect densities in nonpolar III-nitrides in a single regrowth by employing lateral overgrowth from sidewalls of an etched nitride through the mask openings. This method combines the advantages of the well-known single-step LEO¹³ and two-step LEO¹⁴ techniques. SLEO *a*-plane GaN films had threading dislocation (TD) density of $\sim(10^6-10^7) \text{ cm}^{-2}$ and SF density of $\sim(10^3-10^4) \text{ cm}^{-1}$ while planar *a*-plane GaN films had TD density of $\sim 2 \times 10^{10} \text{ cm}^{-2}$ and SF density of $\sim 3.5 \times 10^5 \text{ cm}^{-1}$.

II. EXPERIMENTAL METHODS

To investigate the effect of reduced defect densities on electrical characteristics and to make a relative comparison side-by-side, planar and SLEO *a*-plane GaN templates were co-loaded for regrowth of *n*-doped layers. The planar and SLEO films were grown as described in Refs. 4 and 13, respectively. The SLEO templates were

already highly doped with Si because of the presence of underlying SiO_2 mask media during SLEO overgrowth. To isolate these doped templates, a $\sim 1\text{-}\mu\text{m}$ -thick GaN:Fe insulation layer was grown prior to the Si-doped layer as shown in Fig. 1(a). Following which, a $\sim 0.5\text{-}\mu\text{m}$ GaN:Si layer was grown by varying disilane (Si_2H_6) flows between 0.2 and 1.5 sccm, which corresponded to Si/Ga ratio of 2.75×10^{-5} to 2.06×10^{-4} . For all samples, the growth variables were kept constant at a growth temperature of $1130 \text{ }^\circ\text{C}$, 25 sccm Cp_2Fe and 22 sccm TMGa, 1 slpm NH_3 , and 12 slpm total flows. H_2 was used as carrier gas.

After *n*-type samples were grown with a Thomas Swan close-spaced vertical rotating disk MOCVD reactor, Van der Pauw patterns for Hall measurements and transfer-length method (TLM) patterns [Fig. 1(b)] were defined with photolithography. For *n*-type contacts, Al/Au (300/

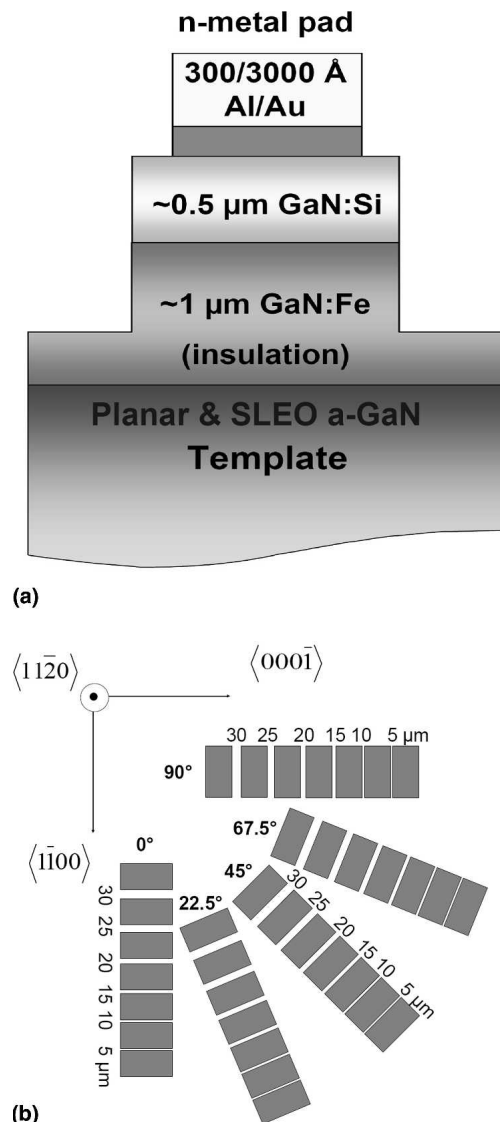


FIG. 1. (a) Schematic of Si-doped Hall and TLM sample structure and (b) processed TLM patterns (courtesy of Mel McLaurin).

3000 Å) was deposited by using an e-beam. Then, square mesa structures, with junction areas of 104 m², were etched with Cl₂-based reactive-ion etching (RIE) and isolated.

The mask was specially designed to measure anisotropic conductivity for 0 to 90° from the designated azimuth. As shown in Fig. 1(b), for nonpolar *a*-(11 $\bar{2}$ 0) plane samples 0° was designated for *m*-(1 $\bar{1}$ 00) azimuth, therefore the *c*-(0001) azimuth was aligned with 90° TLM patterns. The angular dependence of TLM patterns was useful to understand the dynamics between the defects and the electrical characteristics.

The electrical properties of the *n*-type GaN layers were characterized at room temperature by Hall measurements using Van der Pauw patterns and TLM measurements. The Si concentration in the films was determined using secondary-ion mass spectroscopy (SIMS) measurements with high-resolution spectroscopy tools at Charles Evans and Associates (Redwood City, CA).

III. RESULTS AND DISCUSSION

Table I summarizes the SIMS, Hall, and TLM results for planar and SLEO *a*-GaN samples. The SIMS results revealed that both types of samples incorporated similar amounts of Si in the material for a given DiSi flow, and there was a linear increasing trend with increase in DiSi flow. However, the ionization, active carrier concentration, for the SLEO sample was in average ~7% more than planar samples [Fig. 2(c)]. Figures 2(a) and 2(b) show the change in mobility and resistivity values with respect to change in carrier concentrations for planar and SLEO films. As a general trend, mobility values for both planar and SLEO films were linearly increasing with different slope coefficients, and the resistivity values demonstrated an inversely proportional trend with carrier densities. The lowest mobility value observed was ~64 cm²/Vs for SLEO *a*-GaN at Hall concentration of 3.4 × 10¹⁸ cm⁻³. Same mobility value was observed at higher carrier concentration (5.5 × 10¹⁸ cm⁻³) for planar *a*-GaN films. The planar samples with Hall concentrations lower

than 5.5 × 10¹⁸ cm⁻³ were compensated and highly resistive; the SLEO samples, on the other hand, were less compensated while still measuring high resistivity values at lower carrier densities. If the impurities, such as carbon, were held accountable for *n*-type compensation in GaN, then this is the evidence for reduced impurity incorporation in the material due to reduced defect densities.

The highest mobility observed, at the carrier concentration of 1.05 × 10¹⁹ cm⁻³ and the Si/Ga ratio of 2.06 × 10⁻⁴, was 261.12 cm²/Vs for SLEO *a*-GaN and 106.77 cm²/Vs for the planar *a*-plane GaN samples. However, for the same carrier concentration and Si/Ga ratio the carrier compensation for SLEO samples was ~12% less than planar *a*-GaN. At this carrier concentration, the percent ionizations for SLEO and planar films were ~87% and ~75%, respectively. Previously, Craven et al.⁶ obtained the highest mobility at 109 cm²/Vs for a carrier concentration of 1.8 × 10¹⁹ cm⁻³ in planar *a*-GaN samples grown on *a*-plane SiC, which was comparable to what we found for planar *a*-GaN films. Therefore, relative to planar films, SLEO *a*-GaN films had 2.5 times higher mobilities due to reduced compensations and electron scattering sites, such as defects and impurities. In 2005, Kusakabe et al.⁷ reported mobility values of 220 cm²/Vs at carrier concentration of 1.1 × 10¹⁸ cm⁻³ for *n*-doped *a*-plane GaN. Therefore, so far, the mobility value that we report here for *n*-doped nonpolar *a*-plane SLEO GaN samples has been the highest in the literature at a given carrier concentration of 1.05 × 10¹⁹ cm⁻³.

Figure 3 demonstrates the angular dependence of conductivity in planar and SLEO *a*-GaN. In planar samples, the lowest resistivity was obtained along the *c*-azimuth and at 90° apart along the *m*-azimuth the resistivity was highest. When the resistivity values were normalized with respect to highest value, we observed an increasing trend from 0.88 (0° from *c*-azimuth) to 1 (90° from *c*-azimuth). So, independently from the tested TLM area, the percentage drop in resistivity going from *m*-azimuth to *c*-azimuth was 12% for planar *a*-GaN sample [Fig. 3(a)]. However, as Fig. 3(b) shows, in the case of the SLEO sample, the anisotropic trend differs at different

TABLE I. Electrical properties of planar *a*-GaN and SLEO *a*-GaN at various Si doping levels.

	DiSi flow (sccm)	Si/Ga ratio	Si concentration (cm ⁻³)	Hall concentration (cm ⁻³)	Hall mobility (cm ² /V·s)	R- Hall (Ω/□)	R- Sheet (Ω/□)	R- Contact (Ω·mm)
Planar <i>a</i> -GaN	0.2	2.75 × 10 ⁻⁵	4.32 × 10 ⁻¹⁸	NA	NA	NA	NA	NA
	0.5	6.87 × 10 ⁻⁵	6.55 × 10 ⁻¹⁸	5.51 × 10 ⁻¹⁸	62.84	361	412	1.856
	1	1.38 × 10 ⁻⁴	1.03 × 10 ⁻¹⁹	9.02 × 10 ⁻¹⁸	90.46	153.2	162	1.091
	1.5	2.06 × 10 ⁻⁴	1.40 × 10 ⁻¹⁹	1.05 × 10 ⁻¹⁹	106.77	111.5	116.5	1.03
SLEO <i>a</i> -GaN	0.2	2.75 × 10 ⁻⁵	4.33 × 10 ⁻¹⁸	3.4 × 10 ⁻¹⁸	64.18	572.84	600	2.32
	0.5	6.87 × 10 ⁻⁵	6.10 × 10 ⁻¹⁸	5.55 × 10 ⁻¹⁸	127.86	176	183.4	1.368
	1	1.38 × 10 ⁻⁴	9.05 × 10 ⁻¹⁸	8.12 × 10 ⁻¹⁸	230.45	66.8	68	0.9506
	1.5	2.06 × 10 ⁻⁴	1.20 × 10 ⁻¹⁹	1.04 × 10 ⁻¹⁹	261.12	46.03	49	0.9665

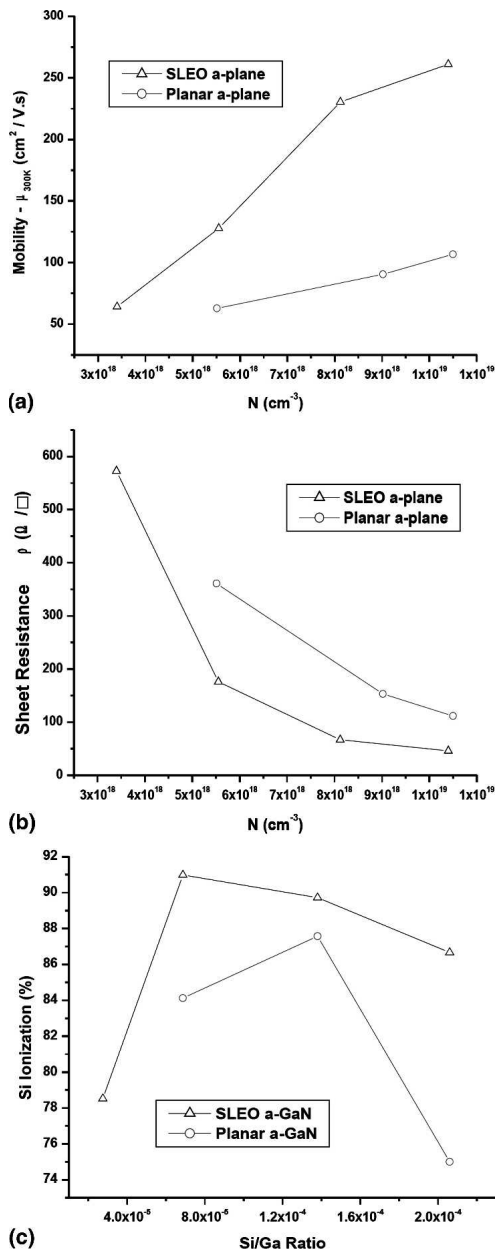


FIG. 2. (a) Change in mobility; (b) change in sheet resistance for planar *a*-GaN and SLEO *a*-GaN with increasing electron concentration levels; and (c) percent Si ionization for planar *a*-GaN and SLEO *a*-GaN.

parts of the same sample with the same Si doping. For example, in TLM area 3 the percentage drop in relative resistivity was ~10%, in TLM area 1 this value was ~45%, and in TLM area 2 there was a scattered trend. Unlike planar films, the defect distribution in the SLEO films was inhomogeneous. The reported defect densities for SLEO films were averaged across the film, so for different areas this value could be either lower or higher than the average. Similarly, we observe a difference in anisotropic conductivity values at different areas of the sample. This varying trend throughout the sample sug-

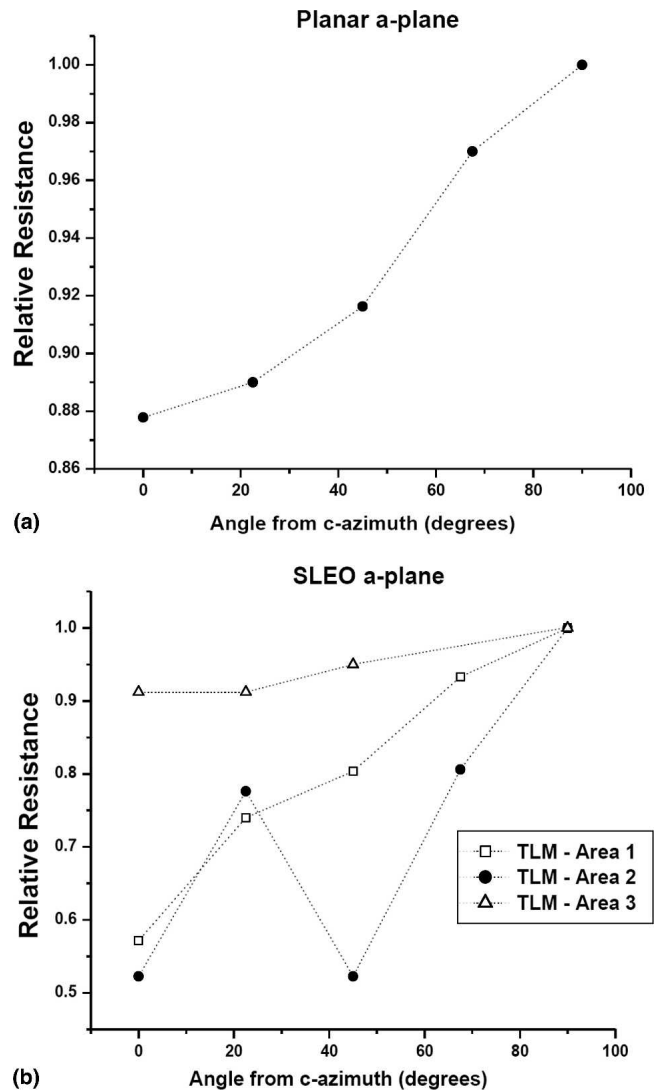


FIG. 3. Angle-dependent resistivity of (a) planar *a*-GaN and (b) SLEO *a*-GaN samples for three different TLM areas.

gested that the anisotropic conductivity was strongly correlated with defects.

In conclusion, we compared *n*-type electrical characteristics of defected planar and reduced defect density SLEO *a*-plane GaN samples at varying Si doping levels. The threading dislocation density of SLEO *a*-plane GaN templates was 3–4 orders of magnitude lower and the stacking fault density was 1–2 orders of magnitude lower compared with the planar *a*-plane GaN templates. The highest mobility observed was 261.12 cm²/Vs at Hall concentration of 1.05×10^{19} cm⁻³ for reduced defect density SLEO material. It exhibited ~2.5 times higher electron mobility with ~12% higher Si ionization compared to planar samples. And in average the carrier concentration was ~7%–8% higher in reduced defect density SLEO films compared with its planar *a*-plane counterparts. The anisotropic conductivity was found to be a function of defect density.

ACKNOWLEDGMENT

The authors acknowledge the support of JST/ERATO and the National Science Foundation for use of Facilities through the Materials Research Science and Engineering Center (MRSEC) program.

REFERENCES

1. P. Waltereit, O. Brandt, M. Ramsteiner, R. Uecker, P. Reiche, and K.H. Ploog: Growth of *m*-plane GaN (1–100) on γ -LiAlO₂ (100). *J. Cryst. Growth* **218**, 143 (2000).
2. A. Bhattacharyya, I. Friel, S. Iyer, T.-C. Chen, W. Li, J. Cabalu, Y. Fedyunin, K.F. Ludwig, Jr., T.D. Moustakas, H.-P. Maruska, D.W. Hill, J.J. Gallagher, M.C. Chou, and B. Chai: Comparative study of GaN/AlGa_xN MQWs grown homoepitaxially on (1 $\bar{1}$ 00) and (0001) GaN. *J. Cryst. Growth* **251**, 487 (2003).
3. G.A. Garret, H. Shen, M. Wraback, B. Imer, B. Haskell, J.S. Speck, S. Keller, S. Nakamura, and S.P. DenBaars: Intensity dependent time-resolved photoluminescence studies of GaN/AlGa_xN multiple quantum wells of varying well width on laterally overgrown *a*-plane and planar *c*-plane GaN. *Phys. Status Solidi A* **5**, 846 (2005).
4. B. Imer, F. Wu, M.D. Craven, J.S. Speck, and S.P. DenBaars: Stability of (1 $\bar{1}$ 00) *m*-plane GaN films grown by metalorganic chemical vapor deposition (MOCVD). *Jpn. J. Appl. Phys.* **45**, 8644 (2006).
5. C.Y. Hwang, M.J. Schurman, W.E. Mayo, Y.C. Lu, R.A. Stall, and T. Salagajj: Effect of structural defects and chemical impurities on hall mobilities in low pressure MOCVD grown GaN. *J. Electron. Mater.* **26**, 243 (1997).
6. M.D. Craven, A. Chakraborty, B. Imer, F. Wu, S. Keller, U.K. Mishra, J.S. Speck, and S.P. DenBaars: Structural and electrical characterization of *a*-plane GaN grown on *a*-plane SiC. *Phys. Status Solidi C* **0(7)**, 2132 (2003).
7. K. Kusakabe and K. Okhawa: Morphological characteristics of *a*-plane GaN grown on *r*-plane sapphire by metalorganic vapor-phase epitaxy. *Jpn. J. Appl. Phys.* **44**, 7931 (2005).
8. N.S. Weimann, L.F. Eastman, D. Doppalapudi, H.M. Ng, and T.D. Moustakas: Scattering of electrons at threading dislocations in GaN. *J. Appl. Phys.* **83**, 3656 (1998).
9. D.C. Look and J.R. Sizelove: Dislocation scattering in GaN. *Appl. Phys. Lett.* **82**, 1237 (1999).
10. E.G. Brazel, M.A. Chin, and V. Narayanamurti: Direct observation of localized high current densities in GaN films. *Appl. Phys. Lett.* **74**, 2367 (1999).
11. K. Leung, A.F. Wright, and E.B. Stechel: Charge accumulation at a threading edge dislocation in gallium nitride. *Appl. Phys. Lett.* **74**, 2495 (1999).
12. B. Imer, F. Wu, S.P. DenBaars, and J.S. Speck: Improved quality (11 $\bar{2}$ 0) *a*-plane GaN with sidewall lateral epitaxial overgrowth. *Appl. Phys. Lett.* **88**, 061908 (2006).
13. M.D. Craven, S.H. Lim, F. Wu, J.S. Speck, and S.P. DenBaars: Threading dislocation reduction via laterally overgrown nonpolar (11 $\bar{2}$ 0) *a*-plane GaN. *Appl. Phys. Lett.* **81**, 1201 (2002).
14. C. Chen, J. Zhang, J. Yang, V. Adivarhan, S. Rai, S. Wu, H. Wang, W. Sun, M. Su, Z. Gong, E. Kuokstis, M. Gaevski, and M.A. Khan: A new selective area lateral epitaxy approach for depositing *a*-plane GaN over *r*-plane sapphire. *Jpn. J. Appl. Phys.* **42**, L818 (2003).